

# On Dissipation-Induced Destabilization and Brake Squeal: A Perspective using Structured Pseudospectra

Patrick Kessler<sup>a</sup> Oliver M. O'Reilly<sup>a,\*</sup> Anne-Lise Raphael<sup>b</sup>  
Maciej Zworski<sup>c</sup>

<sup>a</sup>*Department of Mechanical Engineering, University of California at Berkeley,  
Berkeley, CA 94720, USA*

<sup>b</sup>*Département de Mathématiques Appliquées, École Polytechnique, F-91128  
Palaiseau Cedex, France*

<sup>c</sup>*Department of Mathematics, University of California at Berkeley,  
Berkeley, CA 94720, USA*

---

## Abstract

Numerous linearizations of mechanical systems feature non-normal operators. This is particularly the case in follower force systems, gyroscopic systems and models for squealing brakes. In this paper, it is shown that a pseudospectral analysis can illuminate features of these systems including dissipation-induced destabilization and high eigenvalue sensitivity to parameter variation.

*Key words:* Dissipation-induced destabilization, Follower forces, Brake squeal, Gyroscopic systems, Pseudospectrum

---

## 1 Introduction

A practical mechanic attempting to subdue an energetic and unstable device will immediately think of using dissipation to remove excess energy. In many cases, this strategy is entirely successful, and so it is one of the most surprising results in engineering that dissipation can actually cause instability in some machines. Dissipation-induced destabilization occurs in a wide class of mechanisms including follower force and gyroscopic systems [1–3]. One of the results

---

\* Corresponding author. email: oreilly@berkeley.edu

we will show in this paper is that it also occurs in certain models for brakes, where instability is used as an indicator of brake squeal.

Our goal in this paper is to use the pseudospectral perspective [4,5] to shed light on dissipation-induced destabilization. We put particular emphasis on a variant of the pseudospectrum which we call a structured pseudospectrum, that ends up being useful in the analysis of mechanical systems. Generally, the pseudospectral perspective is well-suited to systems such as brake models, where high sensitivity to parameter variations can make squeal prediction and suppression difficult (see for example references [6,7]). The work presented in this paper also complements existing works on eigenvalue sensitivity in follower force systems and brake models, see for example [1,6,8].

In Section 2 we provide background on pseudospectra, and in Section 3, we introduce structured pseudospectra. These concepts can arise from questions about the behavior of the linear system

$$\dot{x} = Ax, \tag{1}$$

which are usually answered by considering the eigenvalues of  $A$ . The set of these eigenvalues is called the *spectrum* of  $A$  and is denoted  $\text{Spec}(A)$ . Unfortunately there are cases for which  $\text{Spec}(A)$  does a poor job of describing the behavior of (1). These cases motivate the  $\epsilon$ -*pseudospectrum* of  $A$ , which is denoted  $\Lambda_\epsilon(A)$ , and defined by

$$\Lambda_\epsilon(A) = \{\lambda \in \text{Spec}(A + \delta A) \text{ where } \|\delta A\| < \epsilon\}. \tag{2}$$

In this definition,  $\delta A$  can be *any* perturbation to  $A$ , provided its norm<sup>1</sup> is less than  $\epsilon$ . Although consideration of all possible perturbations often is useful, there are many problems in which the perturbations to  $A$  are naturally restricted. For instance when  $A$  corresponds to a mechanical system, the only possible perturbations may correspond to variations of specific parameters such as damping coefficients in follower force systems, and lining stiffness coefficients in models for brakes. In this paper we restrict the structure of  $\delta A$  in (2) and we study the corresponding subset of  $\Lambda_\epsilon(A)$ , which we refer to as a *structured  $\epsilon$ -pseudospectrum*. We show that the structured  $\epsilon$ -pseudospectrum illuminates existing results on dissipation-induced destabilization and brake squeal prediction.

In Section 4 we demonstrate the advantages of the pseudospectral perspective by analyzing the Ziegler pendulum (see Figure 1). Several classical phenomena associated with this system are easy to see using a structured  $\epsilon$ -pseudospectrum in which the perturbations  $\delta A$  in (2) are restricted so that they correspond to changes in the viscous damping of the pendulum joints.

---

<sup>1</sup> In this paper *norm* will always indicate the standard 2-norm.

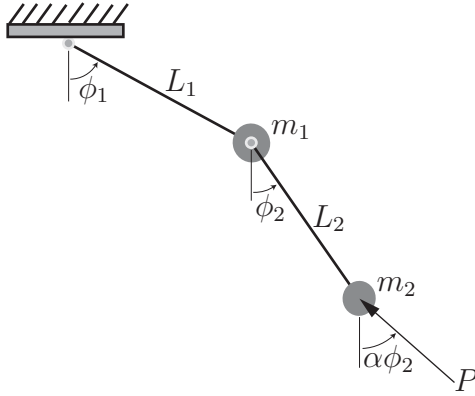


Fig. 1. The Ziegler pendulum consists of two masses connected by rigid links and viscoelastic hinges. The links are oriented by the angles  $\phi_1$  and  $\phi_2$ , and a follower force  $P$  acting on the second mass is oriented by the angle  $\alpha\phi_2$ . The viscoelastic hinges are characterized by stiffness values  $k_1$  and  $k_2$  and damping values  $b_1$  and  $b_2$ . A complete description of this system and its equations of motion is given in Appendix A and also in [2]. In the remainder of the paper we frequently refer to the nondimensionalization of  $P$ , given by  $F = \frac{PL_2}{k_2}$ .

The linearization of the Ziegler pendulum about the trivial equilibrium state has a canonical form that encompasses a large family of mechanical systems, including brake models<sup>2</sup> used in the study of brake squeal. As a result, brake models and follower force systems have similar pseudospectral properties, as we discuss in Section 5.

The phenomenon of dissipation-induced destabilization in mechanical systems has a long history- for references and comments, we refer the reader to [2,10–12]. Relevant background material on brake squeal can be found in the reviews [9,13]. Material on pseudospectra can be found in Trefethen et al. [4,5], and material on structured pseudospectra can be found in references [14–16].

## 2 Background on Pseudospectra

The pseudospectrum of an operator  $A$  can be motivated by questions about the behavior of the associated differential equation  $\dot{x} = Ax$ . We say that the equilibrium  $x = 0$  of the linear system  $\dot{x} = Ax$  is asymptotically stable if all the eigenvalues  $\lambda$  of  $A$  satisfy  $\text{Re}(\lambda) < 0$ . It is indeed true that

$$|x(t)| \leq C \exp\left(t \max_{\lambda \in \text{Spec}(A)} \text{Re}(\lambda)\right) \quad (3)$$

<sup>2</sup> These models date to North [9] (see, for example, [8]).

as  $t \rightarrow \infty$ , with an additional prefactor of  $t^k$  in some cases of multiple eigenvalues. However, if  $A$  is *non-normal*, (that is, if  $A^T A \neq A A^T$ ), then it is well-known that this asymptotic estimate can be highly *non-uniform*, especially if the dimension of  $A$  is large. Non-uniformity means that  $C$  may have to be extremely large for the inequality to hold, clearly decreasing the usefulness of the estimate. This fact encourages further consideration of non-uniformity; we note that non-uniformity is closely related to the behavior of the resolvent  $R(z)$  of the matrix  $A$ .

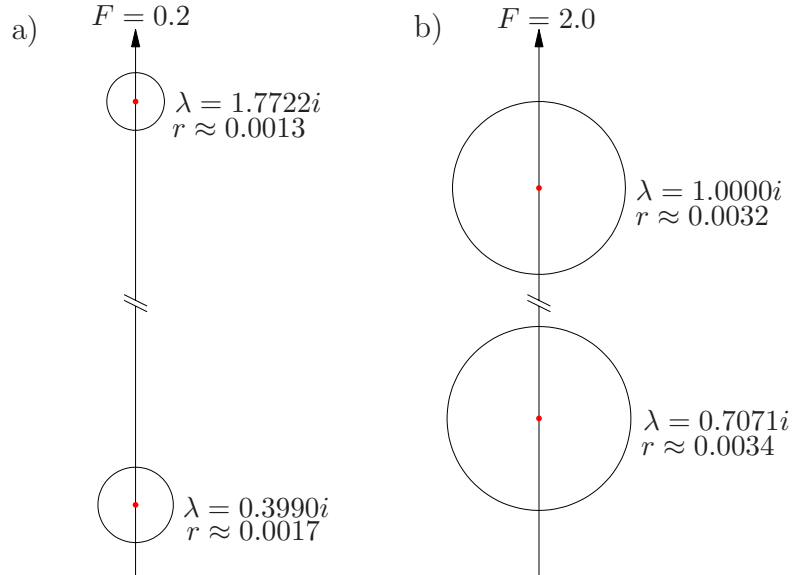


Fig. 2. These images show  $\epsilon$ -pseudospectra (with  $\epsilon=0.001$ ) corresponding to the Ziegler pendulum with the dimensionless force  $F = 0.2$  in a) and  $F = 2.0$  in b). In both a) and b), there are four purely imaginary eigenvalues related by reflective symmetry about the real axis, and so we only show the two that are positive. Each eigenvalue (labeled  $\lambda$ ) is at the center of a roughly circular region (with radius labeled  $r$ ). The  $\epsilon$ -pseudospectrum in a) and b) consists of the union of these circular regions. In both a) and b), a section of the imaginary axis is removed to improve the display. These figures were obtained with the help of EIGTOOL [19].

The resolvent<sup>3</sup> of  $A$  is a matrix valued function defined by

$$R(z) = (zI - A)^{-1}. \quad (4)$$

If  $A$  is normal, then the norm of the resolvent is inversely proportional to the distance between  $z \in \mathbb{C}$  and the spectrum of  $A$ ,

$$\|R(z)\| = \text{dist}(z, \text{Spec}(A))^{-1}. \quad (5)$$

<sup>3</sup> It is useful to note that the resolvent  $R(s)$  is the Laplace transform of the matrix exponential  $e^{tA}$ , and can be expressed as a polynomial function of  $A$  using the Fadeev-Fadeeva formulae [17,18].

The situation is dramatically different however when  $A$  is non-normal. In this case, the norm of the resolvent of  $A$  may be totally unrelated to the distance between  $z$  and the eigenvalues of  $A$ . This motivates the following definition of the  $\epsilon$ -pseudospectrum of  $A$ :

$$\Lambda_\epsilon(A) = \{\lambda \in C \text{ such that } \|R(\lambda)\| > 1/\epsilon\}. \quad (6)$$

This definition is in fact equivalent to (2). The definition in (2) highlights the relation between  $\Lambda_\epsilon(A)$  and spectral instability.

Having defined the  $\epsilon$ -pseudospectrum, we now present an example. In Figure 2 we show  $\epsilon$ -pseudospectra of non-normal operators corresponding to the Ziegler pendulum for different values of  $F$ . As  $F$  increases, the  $\epsilon$ -pseudospectrum grows larger, reflecting an increase in the sensitivity of the system spectrum to perturbations. Furthermore, as  $F$  increases, the operator associated with the Ziegler pendulum becomes increasingly non-normal. We recall that sensitivity to perturbations is characteristic of non-normal systems.

Many of the perturbations  $\delta A$  used to create Figure 2 are not physically realistic (or realizable). To find perturbations that *are* realistic, we need to examine the structure of  $A$ . For a wide class of mechanical systems including the two considered in this paper,  $A$  has the following canonical form:

$$A = \begin{bmatrix} 0 & I \\ -M^{-1}K & -M^{-1}D \end{bmatrix}. \quad (7)$$

Here,  $K$  is a matrix with a symmetric part that corresponds to conservative forces, and with an asymmetric part that contains contributions from either the follower forces or, in the case of brake models, from friction forces.  $M$  is a symmetric positive-definite matrix called the “mass” matrix, and  $D$  is a matrix that represents linear viscous damping. In the absence of damping, (7) corresponds to a reversible dynamical system, but because  $K \neq K^T$ , this system is not Hamiltonian [2]. Loosely speaking, as  $K$  becomes increasingly asymmetric, the matrix  $A$  becomes increasingly non-normal and pseudospectral effects manifest. In follower force systems, this occurs when the magnitude of the follower force increases. In many brake models, this occurs when the friction forces or coefficients of friction increase<sup>4</sup>.

---

<sup>4</sup> See Section 8 of [13] where lumped parameter models for disk brakes are discussed. A detailed discussion of the case of a large degree-of-freedom finite element model can be found in the Appendix of [8].

### 3 Structured Pseudospectra

Motivated by (2), we define a structured  $\epsilon$ -pseudospectrum of the linear operator  $A$  to be

$$\Sigma_\epsilon(A) = \{\lambda \in \text{Spec}(A + \delta A) \text{ such that } \|\delta A\| < \epsilon \text{ and } s(\delta A) > 0\}, \quad (8)$$

where  $s(\delta A) > 0$  indicates that  $\delta A$  satisfies some structural condition. To study the effects of damping and other parameter variations on the mechanical systems (7) of interest, we will examine  $\Sigma_\epsilon(A)$  where

$$A = \begin{bmatrix} 0 & I \\ -M^{-1}K & 0 \end{bmatrix}, \quad (9)$$

and where  $s(\delta A) > 0$  indicates that  $\delta A$  has the following structure

$$\delta A = \begin{bmatrix} 0 & 0 \\ -M^{-1}H & -M^{-1}D \end{bmatrix}, \quad (10)$$

with  $M$  and  $D$  positive definite. Here  $H$  represents variations in the applied forces and stiffnesses. We note that (9) is non-normal when  $K \neq K^T$ .

### 4 Example of a Follower Force System

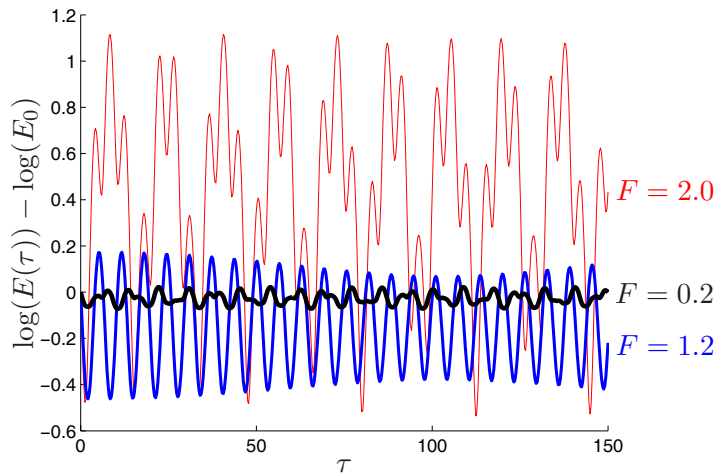
The Ziegler pendulum shown in Figure 1 is a follower force system that experiences dissipation-induced destabilization. This phenomenon is illustrated in Figure 3 where the pendulum position as a function of time is determined by numerically integrating the nonlinear equations given in Appendix A. From this figure we see that for the smaller value of  $F$ , the equilibrium is stable both in the absence and presence of damping. For the larger value of  $F$ , the equilibrium is stable in the absence of damping, but can become unstable when damping is added.

It turns out that dissipation-induced destabilization also occurs in the linearized equations of motion for the Ziegler pendulum, given by  $M\ddot{z} + D\dot{z} + Kz = 0$  where

$$M = \begin{bmatrix} m+2 & 1 \\ 1 & 1 \end{bmatrix}, \quad D = \begin{bmatrix} c_1+c_2 & -c_2 \\ -c_2 & c_2 \end{bmatrix}, \quad K = \begin{bmatrix} 1+\kappa-F & F-1 \\ -1 & 1 \end{bmatrix}. \quad (11)$$

The nondimensional mass, damping, stiffness, and follower force terms  $m$ ,  $c_i$ ,  $\kappa$ , and  $F$  that we use here are defined in Appendix A. The linearized Ziegler

a).



b).

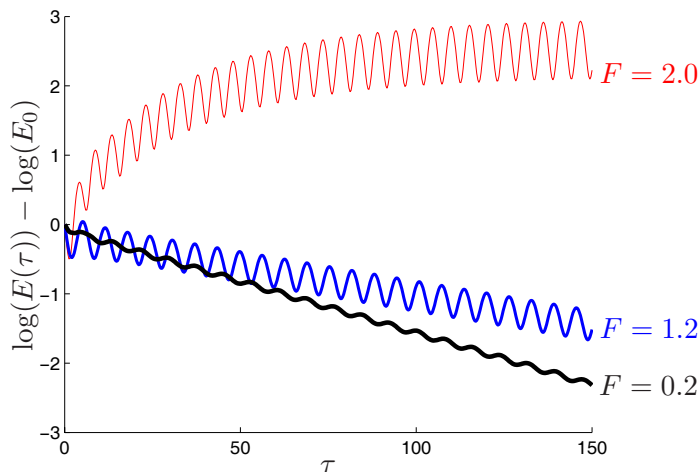


Fig. 3. Simulations showing dissipation-induced destabilization in the Ziegler pendulum when the dimensionless force  $F = 2.0$ . In both a) and b),  $F$  takes on the values 0.2, 1.2 and 2.0, and the logarithm of the normalized total energy  $E$  is plotted as a function of a dimensionless time  $\tau$ . In a), damping is absent, whereas in b), the elements of the damping matrix (11) are  $c_1 = c_2 = 0.1$ . (These nondimensional coefficients are defined in Appendix A.)

equations can be written as  $\dot{x} = Ax$  where  $A$  is the matrix in (7), with  $M$ ,  $D$ , and  $K$  as given above. When  $D$  and  $F$  are zero,  $A$  has a pair of purely imaginary eigenvalues. As  $F$  increases, these eigenvalues move towards each other along the imaginary axis, merging in a reversible Hopf bifurcation<sup>5</sup> when  $F$  is approximately 2.086. In the presence of damping however, the eigenvalues of  $A$  can move into the right half plane for  $F$  as low as 1.2. This is the dissipation-induced destabilization that interests us.

<sup>5</sup> This event is also known as a binary flutter instability.

When  $D = 0$ , the operator  $A$  associated with the Ziegler pendulum is given by (9). The  $\epsilon$ -pseudospectrum of this  $A$  doesn't reveal anything about dissipation-induced destabilization (see Figure 2), although it does show that larger values of  $F$  (which cause  $A$  to be increasingly non-normal) make  $A$  more sensitive to perturbations. We illuminate the system response to dissipation by constructing a structured  $\epsilon$ -pseudospectrum  $\Sigma_\epsilon(A)$  for the system with  $A$  and  $\delta A$  as given in (9) and (10) respectively, with  $H$  in (10) set equal to 0. We generate each  $\delta A$  by constructing a random positive definite  $D$  with unit magnitude, and by then setting

$$\delta A = \begin{bmatrix} 0 & 0 \\ 0 & \beta M^{-1} D \end{bmatrix}, \quad (12)$$

with  $\beta = \frac{\tilde{\epsilon}}{\|M^{-1}D\|}$  for some  $\tilde{\epsilon} \in [0, \epsilon)$ . The random positive definite  $D$  is given by

$$D = \begin{bmatrix} \cos \theta & \sin \theta \\ -\sin \theta & \cos \theta \end{bmatrix} \begin{bmatrix} 1 & 0 \\ 0 & d_1 \end{bmatrix} \begin{bmatrix} \cos \theta & -\sin \theta \\ \sin \theta & \cos \theta \end{bmatrix}, \quad (13)$$

where  $\theta$  and  $d_1$  are random numbers on  $[0, 2\pi]$  and  $(0, 1]$  respectively.

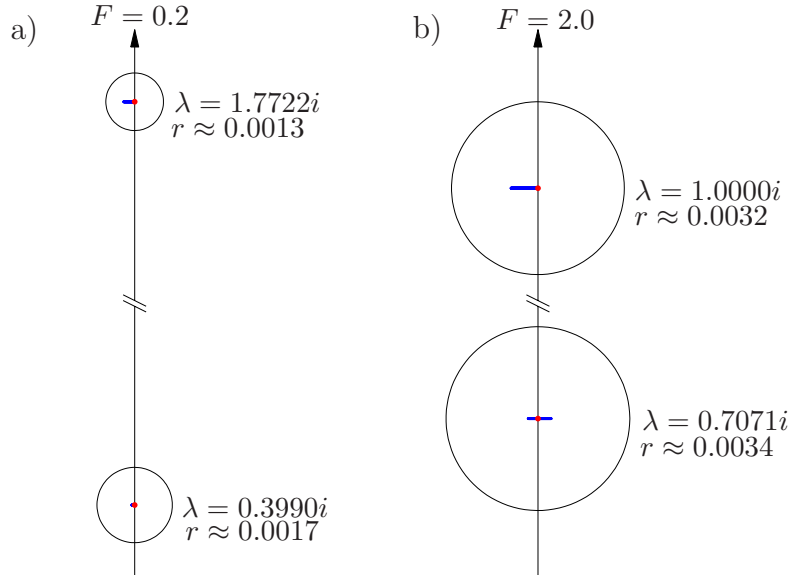


Fig. 4. Here we superpose the structured  $\epsilon$ -pseudospectrum  $\Sigma_\epsilon(A)$  on an exact copy of the  $\epsilon$ -pseudospectrum from Figure 2. In this case,  $\Sigma_\epsilon(A)$  is generated by restricting the perturbations  $\delta A$  to the form (10). This restriction causes the  $\epsilon$ -pseudospectra from Figure 2 to collapse down to the much smaller horizontally-oriented regions at the circle centers. When these smaller regions have a part in the right half plane, (such as when  $F = 2.0$ ), it is possible for the Ziegler pendulum to experience dissipation-induced destabilization. We examine these smaller regions in greater detail in Figures 5 and 6.

In Figure 4 we superpose the structured  $\epsilon$ -pseudospectrum  $\Sigma_\epsilon(A)$  on the regular  $\epsilon$ -pseudospectrum  $\Lambda_\epsilon(A)$  from Figure 2. In Figures 5 and 6, we offer more

images of  $\Sigma_\epsilon(A)$ , in greater detail. It is evident from the first image in Figure 5 that for small  $F$ , dissipation stabilizes the equilibrium. However, as  $F$  gets larger, the non-normality of  $A$  increases and dissipation can induce instability. As is evident from the results for  $F \geq 2.08$ , the destabilization can occur in either pair of eigenvalues.

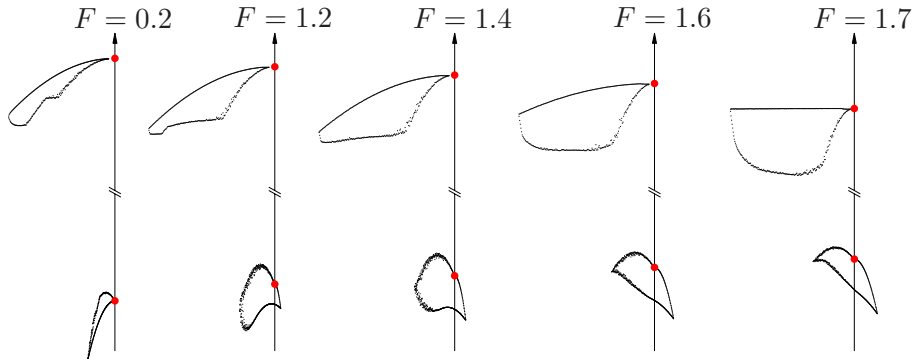


Fig. 5. These images show structured  $\epsilon$ -pseudospectra (with  $\epsilon = 0.001$ ) for the Ziegler pendulum as  $F$  increases through the values 0.2, 1.2, 1.4, 1.6, and 1.7. The structured  $\epsilon$ -pseudospectra are the regions outlined in small dots, the system eigenvalues are the larger dots, and the vertical line in each image is the  $i\mathbb{R}$  axis. As  $F$  increases, the eigenvalues move towards each other along the  $i\mathbb{R}$  axis, and for some  $F$  between 0.2 and 1.2, the structured  $\epsilon$ -pseudospectrum moves into the right half plane. The regions surrounding each eigenvalue are scaled and translated, and data below the real axis is omitted. Actual parameters for these regions are given in Appendix B.

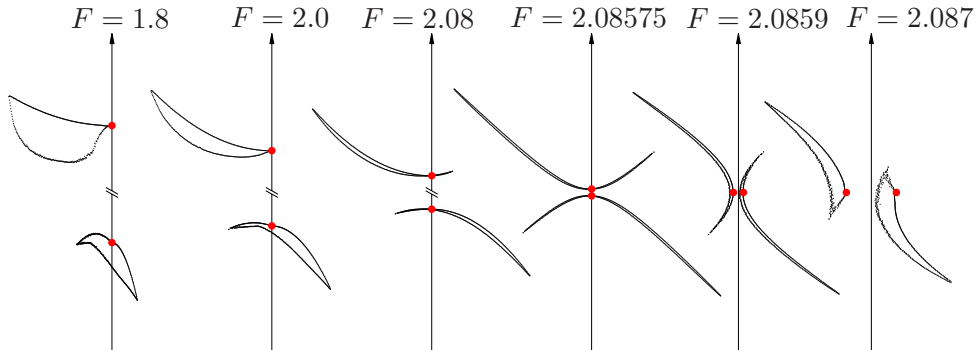


Fig. 6. These images continue the progression from Figure 5, with  $F$  values of 1.8, 2, 2.08, 2.08575, 2.0859, and 2.087. Somewhere between  $F = 2.08575$  and  $F = 2.0859$ , the system eigenvalues coalesce and move off the  $i\mathbb{R}$  axis.

## 5 Brake Squeal

We now consider the usefulness of structured  $\epsilon$ -pseudospectra in predicting brake squeal. As may be surmized from the vast literature on this topic, brake squeal is a fugitive phenomenon for which complete suppression is difficult. Here

we consider a simple brake model (see Figure 7) with a linearization  $A$  that becomes increasingly non-normal as the onset of squeal is approached. As a consequence of this non-normality, the spectrum of  $A$  becomes more sensitive to perturbations, and small changes to the system parameters greatly affect the onset of squeal. Our comments here are in accord with the independent observations on this sensitivity that have appeared in references [6,7]. If we add *large* amounts of dissipation to the system, then the eigenvalues develop negative real parts, and the pseudospectral effects are reduced. This is in agreement with the common practice of using dissipation as a squeal suppression mechanism.<sup>6</sup> Small amounts of damping however may give rise to instability.

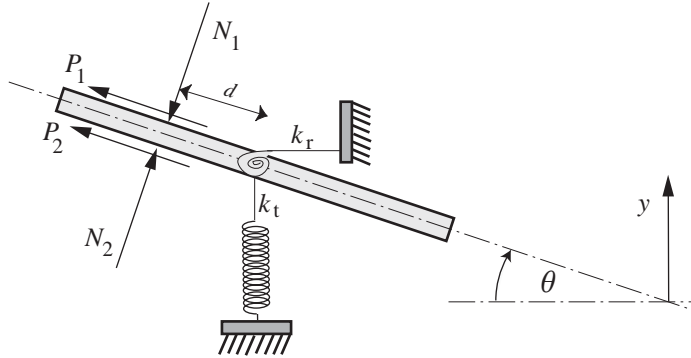


Fig. 7. Schematic of North's two degree-of-freedom model for a disk brake. The brake rotor is represented by the tilted beam, which has a length  $2L$  and a thickness of  $2h$ , while the action of the pads on the rotor is represented by the friction forces  $F_1$  and  $F_2$  and the torsional and linear springs of stiffness  $k_r$  and  $k_t$ , respectively. This figure has been adapted from [9] with some changes in notation.

Our brake model is a discrete two degree-of-freedom system first described by North in [9], (see Figure 7). In this model, the brake rotor is represented by a rigid rod of mass  $m$ , moment of inertia  $I$ , length  $L$  and thickness  $2h$ . The brake pads in contact with the rotor are incorporated into the model by the normal forces  $N_1$  and  $N_2$ , and by the frictional forces  $P_1$  and  $P_2$ . The translational and rotational degrees of freedom of the rod are denoted by  $y$  and  $\theta$ , respectively. To model the stiffness of the rotor, we subject the rod to a torsional spring of stiffness  $k_r$  and a linear spring of stiffness  $k_t$ . The flexibility of the brake pads is included in the model by a linear spring of stiffness  $\frac{k_p}{2}$  for each pad. The normal forces are assumed to be

$$N_1 = \frac{k_p}{2} (y + d\theta) + N_0, \quad N_2 = -\frac{k_p}{2} (y + d\theta) + N_0, \quad (14)$$

where  $N_0$  accounts for a static preload between the brake pads and the rotor, and where  $d$  is the dimension shown in Figure 7. The corresponding expressions

<sup>6</sup> For additional background on squeal suppression mechanisms, see Kinkaid *et al.* [13].

for the frictional forces are

$$P_1 = \mu N_1, \quad P_2 = \mu N_2, \quad (15)$$

where  $\mu$  is a coefficient of friction. The (dimensionless) linearized equations of motion for this model are given by  $M\ddot{z} + D\dot{z} + Kz = 0$  where

$$z = \begin{bmatrix} \frac{y}{d} \\ \theta \end{bmatrix}, \quad M = \begin{bmatrix} 1 & 0 \\ 0 & \frac{1}{md^2} \end{bmatrix},$$

$$K = \begin{bmatrix} 1 + \kappa_p & -\eta + \kappa_p \\ (1 + \sigma)\kappa_p & (1 + \sigma)\kappa_p + \kappa_r \end{bmatrix}, \quad (16)$$

and where  $D$  is a positive definite matrix representing the effects of damping. The dimensionless parameters in these matrices are

$$\kappa_p = \frac{k_p}{k_t}, \quad \kappa_r = \frac{k_r}{d^2 k_t}, \quad \sigma = \frac{\mu h}{d}, \quad \eta = \frac{2\mu N_0}{k_t d}, \quad (17)$$

where the frequency  $\sqrt{\frac{k_t}{m}}$  is used to nondimensionalize time. The system equations of motion can be written as  $\dot{x} = Ax$  where  $A$  is given by the canonical form (7), just as it was for the Ziegler pendulum. Recall that  $A$  is non-normal when  $K \neq K^T$ , which in our system occurs when

$$\mu + \sigma\kappa_p \neq 0 \iff \mu \left( \frac{k_p}{k_t} \frac{h}{d} + 1 \right) \neq 0 \quad (18)$$

This condition always holds because the friction coefficient  $\mu$  never is zero. The structured  $\epsilon$ -pseudospectra for this system are qualitatively similar to those of the Ziegler pendulum, with the friction coefficient  $\mu$  in the brake model analagous to the follower force  $F$  in the Ziegler pendulum. The introduction of *small* amounts of damping can cause the system eigenvalues to move into the right half plane, for lesser friction coefficient values than those needed to reach the reversible Hopf bifurcation in the case when no damping is present.

## 6 Concluding Remarks

We have used structured pseudospectra to illustrate the presence of dissipation-induced destabilization in follower force systems and brake models. Related results also apply for gyroscopic systems, but are so similar that we don't present them here.<sup>7</sup> We point out that non-normal matrices which have a

<sup>7</sup> A good system to explore these results is Example 4.6.1 in [12].

more general structure than (7) can be found in the literature (see, e.g., reference [7]), and that a structured pseudospectral analysis can also be performed for them.

## Acknowledgements

This research was partially supported by grants from the Center for Pure and Applied Mathematics at the University of California at Berkeley. The work of Maciej Zworski was partially supported by grant number DMS-0200732 from the National Science Foundation.

## A Equations of Motion for the Ziegler Pendulum

The pendulum system shown in Figure 1 consists of a mass  $m_1$  attached by a link  $L_1$  to a fixed base, and a mass  $m_2$  attached by a link  $L_2$  to the mass  $m_1$ . The links  $L_1$  and  $L_2$  make angles  $\phi_1$  and  $\phi_2$  respectively with a fixed line of reference. The points of attachment are viscoelastic hinges, endowed with torsional stiffness and damping. We quantify the torsional stiffness at the first and second hinges by the coefficients  $k_1$  and  $k_2$  respectively. These coefficients have units of [force]x[distance]. The damping coefficients associated with the first and second hinges are denoted  $b_1$  and  $b_2$  respectively, and have units of [force]x[distance]x[time]. A follower force of magnitude  $F$  acts on  $m_2$  at an angle  $\alpha\phi_2$  with respect to the line of reference from before. For good measure we include gravity  $g$  acting on both masses in the direction of the line of reference.

We first use the frequency  $\nu = \sqrt{\frac{k_2}{L_2^2 m_2}}$  to establish the following nondimensional values:

$$\begin{aligned} F &= \frac{PL_2}{k_2}, & \kappa &= \frac{k_1}{k_2}, & l &= \frac{L_1}{L_2}, & m &= \frac{m_1}{m_2} - 1, \\ \gamma &= \frac{g}{\nu^2}, & c_1 &= \frac{b_1\nu}{k_2}, & c_2 &= \frac{b_2\nu}{k_2}, & \tau &= t\nu. \end{aligned} \quad (\text{A.1})$$

With the understanding that a superscripted dot indicates differentiation with

respect to  $\tau$ , the Ziegler Pendulum equations of motion are given by

$$\begin{aligned}
& \begin{bmatrix} l^2(m+2) & l \cos(\phi_1 - \phi_2) \\ l \cos(\phi_1 - \phi_2) & 1 \end{bmatrix} \begin{bmatrix} \ddot{\phi}_1 \\ \ddot{\phi}_2 \end{bmatrix} = \\
& l \sin(\phi_1 - \phi_2) \begin{bmatrix} -\dot{\phi}_2^2 \\ \dot{\phi}_1^2 \end{bmatrix} + \begin{bmatrix} -(\kappa+1) & 1 \\ 1 & -1 \end{bmatrix} \begin{bmatrix} \dot{\phi}_1 \\ \dot{\phi}_2 \end{bmatrix} + F \begin{bmatrix} \sin(\phi_1 - \alpha\phi_2) \\ l^{-1} \sin((1-\alpha)\phi_2) \end{bmatrix} \\
& + \begin{bmatrix} -(c_1+c_2) & c_2 \\ c_2 & -c_2 \end{bmatrix} \begin{bmatrix} \dot{\phi}_1 \\ \dot{\phi}_2 \end{bmatrix} - \gamma \begin{bmatrix} l(m+2) \sin \phi_1 \\ \sin \phi_2 \end{bmatrix}. \tag{A.2}
\end{aligned}$$

The nondimensional kinetic, spring potential, and gravitational potential energies of the system are

$$\begin{aligned}
KE &= \frac{1}{2} l^2 (m+2) \dot{\phi}_1^2 + \frac{1}{2} \dot{\phi}_2^2 + l \dot{\phi}_1 \dot{\phi}_2 \cos(\phi_1 - \phi_2), \\
PE_s &= \frac{1}{2} (\kappa \phi_1^2 + (\phi_2 - \phi_1)^2), \\
PE_g &= -\gamma (m+2) l \cos \phi_1 - \gamma \cos \phi_2. \tag{A.3}
\end{aligned}$$

With  $\alpha = 1$  and  $\gamma = 0$ , the system linearization about zero is given by

$$M \begin{bmatrix} \ddot{\phi}_1 \\ \ddot{\phi}_2 \end{bmatrix} + D \begin{bmatrix} \dot{\phi}_1 \\ \dot{\phi}_2 \end{bmatrix} + K \begin{bmatrix} \phi_1 \\ \phi_2 \end{bmatrix} = 0, \tag{A.4}$$

where

$$M = \begin{bmatrix} m+2 & 1 \\ 1 & 1 \end{bmatrix}, \quad D = \begin{bmatrix} c_1+c_2 & -c_2 \\ -c_2 & c_2 \end{bmatrix}, \quad K = \begin{bmatrix} 1+\kappa-F & F-1 \\ -1 & 1 \end{bmatrix}. \tag{A.5}$$

## B Data From Figures 5 and 6

Table 1 gives the eigenvalues and structured  $\epsilon$ -pseudospectra dimensions from Figures 5 and 6. For each value of  $F$ , the structured  $\epsilon$ -pseudospectrum consists of four distinct regions in  $\mathbb{C}$ , each containing one of the system eigenvalues. We identify each such region  $\Psi$  by the eigenvalue it contains. The structured pseudospectrum is symmetric with respect to the real axis, and so we only give data above the real axis.

| F       | Re( $\lambda$ ) | Im( $\lambda$ ) | min(Re( $\Psi$ )) | $\Delta$ Re( $\Psi$ ) | min(Im( $\Psi$ )) | $\Delta$ Im( $\Psi$ ) |
|---------|-----------------|-----------------|-------------------|-----------------------|-------------------|-----------------------|
| 0.20000 | -9.496656e-18   | 1.772232e+00    | -4.918268e-04     | 4.626542e-04          | 1.772232e+00      | 8.034621e-08          |
| 0.20000 | 1.135801e-16    | 3.989923e-01    | -1.253187e-04     | 1.249762e-04          | 3.989923e-01      | 2.221254e-08          |
| 1.20000 | -1.949384e-17   | 1.434196e+00    | -5.276500e-04     | 5.026811e-04          | 1.434196e+00      | 8.058873e-08          |
| 1.20000 | 1.949384e-17    | 4.930336e-01    | -1.474492e-04     | 1.723291e-04          | 4.930336e-01      | 2.181407e-08          |
| 1.40000 | 6.884011e-17    | 1.351373e+00    | -5.503930e-04     | 5.273948e-04          | 1.351373e+00      | 7.829293e-08          |
| 1.40000 | -4.108453e-17   | 5.232507e-01    | -1.619412e-04     | 2.070492e-04          | 5.232507e-01      | 2.859811e-08          |
| 1.60000 | 3.928148e-17    | 1.258741e+00    | -5.887940e-04     | 5.645737e-04          | 1.258741e+00      | 8.145434e-08          |
| 1.60000 | -1.152590e-17   | 5.617572e-01    | -1.866597e-04     | 2.697304e-04          | 5.617571e-01      | 6.534549e-08          |
| 1.70000 | 2.679640e-18    | 1.206970e+00    | -6.204038e-04     | 6.006905e-04          | 1.206970e+00      | 8.897478e-08          |
| 1.70000 | -2.679640e-18   | 5.858529e-01    | -2.059099e-04     | 3.210697e-04          | 5.858528e-01      | 1.069690e-07          |
| 1.80000 | 2.123300e-17    | 1.149652e+00    | -6.706411e-04     | 6.505671e-04          | 1.149652e+00      | 1.785604e-07          |
| 1.80000 | 6.522575e-18    | 6.150617e-01    | -2.295368e-04     | 3.949867e-04          | 6.150616e-01      | 1.945922e-07          |
| 2.00000 | 1.804112e-16    | 1.000000e-00    | -9.831250e-04     | 9.758750e-04          | 9.999998e-01      | 1.562333e-06          |
| 2.00000 | -4.483593e-17   | 7.071068e-01    | -3.500000e-04     | 8.281930e-04          | 7.071053e-01      | 1.572187e-06          |
| 2.08000 | -6.278791e-16   | 8.797905e-01    | -3.032270e-03     | 3.559450e-03          | 8.797900e-01      | 9.897194e-05          |
| 2.08000 | 5.723679e-16    | 8.037218e-01    | -9.253781e-04     | 3.424958e-03          | 8.036232e-01      | 9.897771e-05          |
| 2.08575 | 3.955170e-15    | 8.439200e-01    | -1.032975e-02     | 1.502420e-02          | 8.439149e-01      | 7.460492e-03          |
| 2.08575 | -4.024558e-15   | 8.378837e-01    | -5.140275e-03     | 1.484115e-02          | 8.304282e-01      | 7.460505e-03          |
| 2.08590 | 5.328282e-03    | 8.408795e-01    | 5.097472e-03      | 5.618368e-03          | 8.312490e-01      | 1.347916e-02          |
| 2.08590 | -5.328282e-03   | 8.408795e-01    | -1.120838e-02     | 5.860394e-03          | 8.368811e-01      | 1.352532e-02          |
| 2.08700 | 1.741811e-02    | 8.407160e-01    | 1.717581e-02      | 9.079214e-04          | 8.350055e-01      | 7.293936e-03          |
| 2.08700 | -1.741811e-02   | 8.407160e-01    | -1.857042e-02     | 1.133566e-03          | 8.390573e-01      | 7.310464e-03          |

Table 1: Eigenvalues and structured  $\epsilon$ -pseudospectra dimensions from Figures 5 and 6. In this table,  $\Delta$ Re( $\Psi$ ) denotes  $\max(\text{Re}(\Psi)) - \min(\text{Re}(\Psi))$ , and  $\Delta$ Im( $\Psi$ ) denotes  $\max(\text{Im}(\Psi)) - \min(\text{Im}(\Psi))$ .

## References

- [1] O.N.Kirillov and A.O.Seyranian, *The effect of small internal and external damping on the stability of distributed non-conservative systems*, Journal of Applied Mathematics and Mechanics, **69**, (2005), 529–552.
- [2] O. M. O’Reilly, N. K. Malhotra and N. S. Namachchivaya, *Some aspects of destabilization of the equilibria of reversible dynamical systems with application to follower forces*, Nonlinear Dynamics, **10** (1996), 63–87.
- [3] H. Ziegler, *Die Stabilitätskriterien der Elastomechanik*, Ingenieur Archiv, **20**(1), (1952), 49–56.
- [4] L.N. Trefethen and M. Embree, *Spectra and Pseudospectra: The Behaviour of Non-Normal Matrices and Operators*, Princeton University Press, 2005.

- [5] L.N. Trefethen, *Pseudospectra of linear operators*, SIAM Review, **39** (1997), 383-400.
- [6] J. Huang, C. M. Krousgrill and A. K. Bajaj, *Modeling of automotive drum brakes for squeal and parameter sensitivity analysis*, Journal of Sound and Vibration, **289**, (2006), 245–263.
- [7] U. Von Wagner, D. Hochlenert and P. Hagedorn, *Minimal models for the explanation of disk brake squeal*, Journal of Sound and Vibration, Submitted for publication 2005.
- [8] Y.S. Lee, P. C. Brooks, D. C. Barton and D. A. Crolla, *A predictive tool to evaluate disc brake squeal propensity. Part 2: System linearization and modal analysis*, International Journal of Vehicle Design, **31**(3) (2003), 309–329.
- [9] M. R. North, *Disc brake squeal*, In Braking of Road Vehicles, pp. 169–176, Automobile Division of the Institution of Mechanical Engineers, Mechanical Engineering Publications Limited, London, England, 1976.
- [10] A. Bloch, P. S. Krishnaprasad, J. E. Marsden and T. Ratiu, *Dissipation induced instabilities*, Annales De L’Institut H. Poincaré: Analyse Non Linéaire. **11** (1994), 37–90 .
- [11] G. Haller, *Gyroscopic stability and its loss in systems with two essential coordinates*, International Journal of Nonlinear Mechanics, **27**(1), (1992), 113–127.
- [12] D. J. Inman, *Vibration with Control, Measurement and Stability*, Prentice Hall, Englewood Cliffs, New Jersey (1989).
- [13] N. M. Kinkaid, O. M. O’Reilly and P. Papadopoulos, *Automotive disk brake squeal*, Journal of Sound and Vibration, **267**(1), (2003), 105–166.
- [14] J. Kozánek, *Resolvent of matrix polynomials, pseudospectra and inversion problems*. Selçuk Journal of Applied Mathematics, **3**(1), (2002).
- [15] F. Tisseur and N. J. Higham, *Structured pseudospectra for polynomial eigenvalue problems with applications*, SIAM Journal of Matrix Analysis and Applications, **23**(1), (2001), 187–208.
- [16] T. Wagenknecht and J. Agarwal, *Structured pseudospectra in structural engineering*, Preprint: University of Bristol <http://seis.bris.ac.uk/enxtw/> International Journal for Numerical Methods in Engineering, to appear.
- [17] S.-H. Hou, *A Simple Proof of the Leverrier–Faddeev characteristic polynomial algorithm*, SIAM Review, **40**(3), (1998), 706–709.
- [18] L. A. Zadeh and C. A. Desoer, *Linear Systems Theory: The State Space Approach*, McGraw-Hill, New York (1963).
- [19] T. G. Wright, *EIGTOOL: A graphical tool for nonsymmetric eigenproblems*. Oxford University <http://www.comlab.ox.ac.uk/pseudospectra/eigtool/>.